Idealized storm evolution and the difference between the eastern and the western North Pacific calculated by an atmosphere-wave-ocean coupled model

Akiyoshi Wada

Meteorological Research Institute, Tsukuba, Ibaraki, 305-0052, JAPAN

1. Introduction

Previously, Wada et al. (2012) reported that the relationship between maximum tropical cyclone (TC) intensity and tropical cyclone heat potential (TCHP) accumulated from the genesis to first reaching the minimum central pressure (MCP) differed between the eastern and western Pacific. Relatively high accumulated TCHP was required for reaching a certain value of MCP in the western Pacific. In other words, TCs can intensify in the eastern Pacific more easily. In order to verify the difference of TC evolution and the maximum intensity, idealized numerical experiments were performed by using an atmosphere-wave-ocean coupled model (Wada et al., 2010) with an idealized TC-like vortex (see Wada, 2009).

2. Model and experimental design

The atmospheric initial conditions were provided by the global objective analysis of the Japan Meteorological Agency on a horizontal grid with a spacing of approximately 20 km. The date at the initial integration time was 00 UTC on 14 September in 2009. The computational domain centered at 16.0˚N and 148.8˚E in the experiment for the western North Pacific storm, and at 16.0˚N and 108.5˚W for the eastern North Pacific storm. At that time, Typhoon Choi-wan existed around the center position in the western North Pacific, whereas there was no TC in the eastern North Pacific. Figure 1 shows vertical profiles of potential temperature, equivalent potential temperature and saturated equivalent potential temperature in the eastern North Pacific (Fig. 1a) and those in the western North Pacific (Fig. 1b) averaged over the computational domain for each experiment. The middle troposphere was relatively dry in the eastern North Pacific at the initial time. TC-like vortex calculated based on Wada (2009) was introduced at the initial time.

A coupled atmosphere-wave-ocean model based on a nonhydrostatic atmosphere model, the third generation ocean wave model and a multilayer ocean model (Wada et al., 2010) was used in this study. The time step was 6 seconds. The domain covered 1200 x 1200 km^2 with a horizontal grid spacing of 1.5 km. The number of the vertical layer was 40 with variable intervals from 40 m at the lowermost layer near the surface to 1180 m at the uppermost layer, and a top height of nearly 23 km. The standard longitude of map projection for Lambert conformal projection was 120˚W in the experiment for the eastern North Pacific storm, while it was 140 ˚E for the western North Pacific storm. Th e Coriolis parameter was assumed to the constant (4.0 x 10^{-5}). The environment was assumed to be motionless.

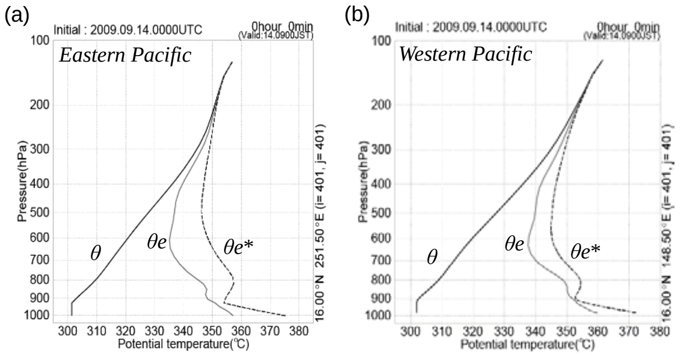

Figure 1 Initial vertical atmospheric profiles of potential temperature (θ: black solid line), equivalent potential temperature (θe: gray solid line) and saturated equivalent potential temperature ($\theta e*$: dashed line) (a) in the eastern North Pacific and (b) in the western North Pacific.

Table 1 shows the list of numerical experiments. A half were performed by the coupled model, while the rest was performed by the atmosphere model. Two roughness schemes, Taylor and Yelland (2001) and Smith (1992) were respectively used for each experiment. In all experiments, a sea spray parameterization (Bao et al. 2000) was used. The sensitivity of rainpower effect (Sabuwala et al., 2015) on the evolution of TC-like vortex was additionally examined in the series of numerical experiments. The program for the effect was coded in the atmospheric boundary layer scheme on the atmosphere model.

Table1 List of numerical experiments.

Acronyms	Area	Ocean/Wave	Roughness length scheme	Rainpower effect
EAST_TY_A	Eastern Pacific	No	Taylor and Yelland (2001)	No
EAST_TY_AWO	Eastern Pacific	Yes	Taylor and Yelland (2001)	No
EAST_SM_A	Eastern Pacific	No	Smith(1992)	No
EAST_SM_AWO	Eastern Pacific	Yes	Smith(1992)	No
WEST_TY_A	Western Pacific	No	Taylor and Yelland (2001)	No
WEST_TY_AWO	Western Pacific	Yes	Taylor and Yelland (2001)	No
WEST_SM_A	Western Pacific	No	Smith(1992)	No
WEST_SM_AWO	Western Pacific	Yes	Smith(1992)	No
EAST_TY_A_RPW	Eastern Pacific	No	Taylor and Yelland (2001)	Yes
EAST_TY_AWO_RPW	Eastern Pacific	Yes	Taylor and Yelland (2001)	Yes
WEST_TY_A_RPW	Western Pacific	No	Taylor and Yelland (2001)	Yes
WEST_TY_AWO_RPW	Western Pacific	Yes	Taylor and Yelland (2001)	Yes

3. Results and concluding remarks

Figure 2 shows the time series of calculated maximum wind speeds at 20-m height for the idealized vortex in the eastern North Pacific (Fig. 2a) and for the vortex in the western North Pacific (Fig. 2b). The calculated vortex intensified more rapidly in the eastern North Pacific than in the western North Pacific. The intensification was irrespective of the roughness length scheme. There was a notable difference in the wind speed variation: the intensification showed periodic fluctuations in the western North Pacific. The ocean coupling did affect the maximum wind speed in the eastern

North Pacific, while the coupling effect depended on the roughness length scheme in the western North Pacific. The rainpower effect helped lessen the vortex intensity without considering the ocean coupling effect, consistent with Sabuwala et al. (2015). However, the lessening effect was relatively small in the numerical experiments performed by the coupled model. Interestingly, the maximum wind speeds in the rainpower experiments did not decrease during the mature phase.

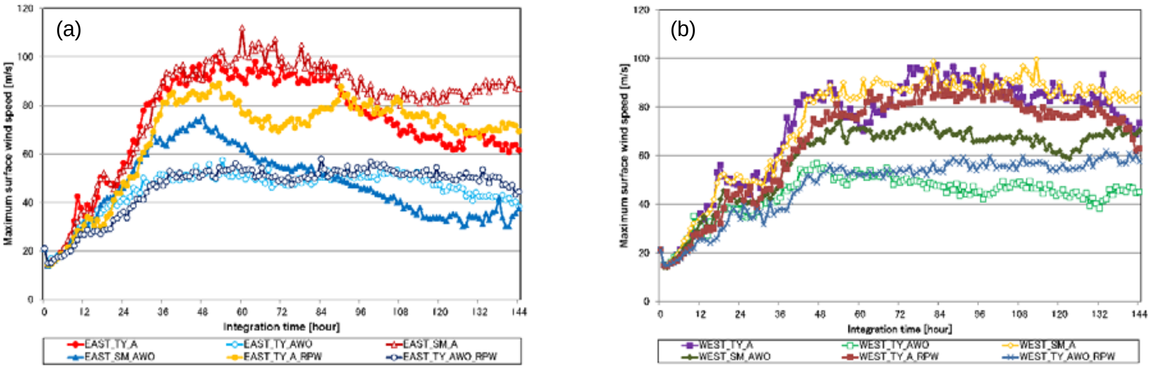

Figure 2 Time series of calculated maximum wind speeds at 20-m height (a) for the storm in the eastern North Pacific and (b) for the storm in the western North Pacific.

Figure 3 shows calculated storm positions relative to the initial position for the idealized vortex in the eastern North Pacific (Fig. 3a) and for the vortex in the western North Pacific (Fig. 3b). The vortex moved northwestward during the intensification phase (Fig. 2). It changed the moving direction cyclonically in the northern hemisphere. In the eastern North Pacific, the vortex's track was greatly sensitive to the roughness length scheme particularly in the experiment with the coupled model. In addition, the rainpower effect also affected the vortex's track. On the other hand, the effects of the roughness length scheme, ocean coupling and rainpower effect were relatively weak in the western North Pacific.

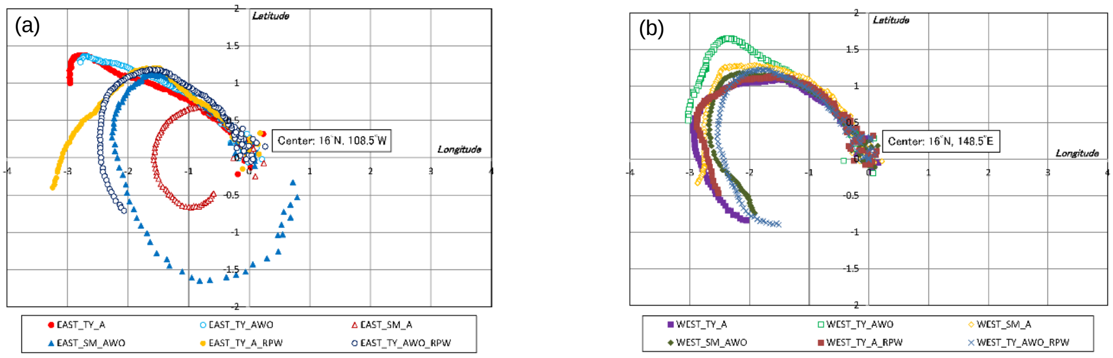

Figure 3 Storm positions relative to the initial position (a) for the storm in the eastern North Pacific and (b) for the storm in the western North Pacific.

The result of numerical experiments is consistent with Wada et al (2012): The vortex can intensify in the eastern Pacific more easily. However, the difference is relatively small in the numerical experiments by the coupled model. The difference of thermodynamic profiles does affect the intensity change of the vortex during the intensification phase particularly after the spin-up ends, around 18-hour integration time. The difference of the vortex's intensity might lead to the difference of the vortex's trajectory after the intensification phase. The sensitivity of the roughness length scheme, ocean coupling and rainpower effect to the trajectory shows various differences. For understanding the processes associated with the differences, the structural change and the asymmetric feature of the vortex should be examined in the future.

It should be noted that calculated mass fields such as the field of calculated sea-level pressures had an increasing or decreasing bias through the integration. The total mass in the computational domain was not conserved in this study. Apart from the necessity of the conservation, the configuration of the numerical experiments should be carefully examined to find a definite difference among the results of numerical simulations. In that sense, this report only shows a preliminary result of sensitivity numerical experiments.

Acknowledgement
This work was supported by MEXT KAKENHI Grant Number 15K05292.

References

Bao, J.-W., J. M. Wilczak, J.-K. Choi and L. H. Kantha (2000). Numerical simulations of air-sea interaction under high wind conditions using a coupled model: A study of hurricane development. Mon. Wea. Rev., 128, 2190-2210.
Sabuwala, T, G Gioia, and P Chakraborty (2015). Effect of rainpower on hurricane intensity. Geophys. Res. Lett., 42, 3024–3029.
Smith, S. D., et al. (1992). Sea surface wind stress and drag coefficients: The HEXOS results. Boundary Layer Meteorol., 60, 109–142.
Taylor, P. K., and M. J. Yelland (2001). The dependence of sea surface roughness on the height and steepness of the waves. J. Phys. Oceanogr., 31, 572–590.
Wada, A. (2009). Idealized numerical experiments associated with the intensity and rapid intensification of stationary tropical cyclone-like vortex and its relation to initial sea-surface temperature and vortex-induced sea-surface cooling, J. Geophys. Res. Atmos., 114, D18111.
Wada, A., N. Kohno and Y. Kawai (2010). Impact of wave-ocean interaction on Typhoon Hai-Tang in 2005. SOLA, 6A, 13-16.
Wada, A., N. Usui, and K. Sato (2012). Relationship of maximum tropical cyclone intensity to sea surface temperature and tropical cyclone heat potential in the North Pacific Ocean. J. Geophys. Res. Atmos., 117, D11118.